

Optical investigation of a -Si:H/ a -SiN_x:H superlattices

S. Kalem*

Department of Physics, The University of Sheffield, Sheffield S3 7RH, United Kingdom

(Received 15 April 1987; revised manuscript received 30 December 1987)

Optical properties of hydrogenated amorphous-silicon–amorphous-silicon-nitride (a -Si:H/ a -SiN_x:H) superlattices ($x = 1.1$) with a -Si:H sublayer thicknesses d_S as small as 11 Å have been investigated by photothermal deflection spectroscopy combined with the transmission and photoluminescence measurements. Changes in the optical band gap, Urbach energy, and defect-state absorption were observed for $d_S < 30$ Å and studied in detail in order to clarify the origin of the size effects in these structures. In the lowest-thickness superlattices, the room-temperature luminescence consists of two emission bands at 1.3 and 1.46 eV, which we ascribe to hydrogen-rich and nitrogen-rich interfaces, respectively. The properties of these amorphous superlattices have been compared with those of hydrogen-rich a -Si:H deposited at low temperatures and a -SiN_x:H alloys ($0 < x < 1.1$) contaminated deliberately by nitrogen.

I. INTRODUCTION

Amorphous superlattices consisting of hydrogenated amorphous silicon (a -Si:H) layers alternating with hydrogenated amorphous silicon nitride (a -SiN_x:H) are the subject of considerable attention because of their interesting physical properties^{1–4} and technological importance.^{5,6} In these structures, when a -Si:H thickness is reduced below about 40 Å, sharp changes have been observed in the optical and electronic properties and attributed to the crystalline superlattice-like confinement effects.^{1,7,8} However, despite several studies,^{9–12} quantum confinement of charge carriers in the lower band-gap layers has not yet been unambiguously identified in these amorphous superlattice systems. Because of the lack of periodicity, the pronounced structures seen in the optical spectra of the crystalline superlattices are absent in the amorphous case. Size effects are clearly seen, but they may be due to chemical contamination of the quantum-well layer or to interface defects. Most of the studies of optical and electronic properties have concentrated on the nature of the interfaces.^{13,14} X-ray diffraction and transmission-electron-microscopy measurements have demonstrated the existence of the alternating layer structures^{1,15} and an interface roughness of about 10–15 Å (almost the sensitivity range of the measurements) has been deduced from different spectroscopic techniques.^{16,17} Also, the existence of built-in electric fields due to charged interface defects and an excess of hydrogen and nitrogen content in the lowest-thickness samples have been reported.^{13,18} Thus the complex structure of the interfaces should play an important role in the determination of the physical properties. But little is known about the composition of the well layer with a thickness of less than about 40 Å, the thickness which corresponds to the onset of the quantum size effects. In fact, this layer determines optical transitions and its minimum contamination, for example by alloying with nitrogen, should result in the changes similar to the confinement effect. In a plasma discharge, it is possible that the residual ammonia

molecules tend to redeposit during the growth of the a -Si:H layer and a part of a a -Si:H may be transferred to a nitride during the growth of the a -SiN_x:H because of the reactive nature of the plasma. The first direct evidence for the presence of nitrogen in the well layer has been obtained from Rutherford backscattering analysis of a structure with 50 Å a -Si:H over 50 Å nitride.¹⁹ Possible contamination of the a -Si:H layer has also been considered by other groups^{20,21} from optical and electrical measurements. But it has not yet been possible to distinguish between interface, contamination, and confinement effects in these superlattices.

Optical measurements are of importance since they have been successfully used to provide direct evidence for bound states in crystalline low-dimensional confined systems.⁸ In amorphous superlattices, as the fine structure is absent, the blue shift of the fundamental absorption edge and of the photoluminescence (PL) peak energy has been used as evidence of the level shift. So far absorption measurements on these structures report shifts of the gap to higher energies for layer thicknesses below about 40 Å. Nevertheless, no systematic study of the optical properties of these superlattice structures has been done until now. In this work, we have studied in detail the below- and above-gap absorption, and photoluminescence properties of a -Si:H/ a -SiN_x:H superlattices using photothermal deflection spectroscopy (PDS),²² the transmission method, and photoluminescence at room temperature. Because of the high sensitivity of the PDS technique, we could precisely measure the low-level absorption processes in these thin films with thicknesses of less than 0.3 μm down to 0.8 eV. We present the thickness-induced changes in all the characteristic parameters of the material, such as Urbach energy, optical band gap, as well as defect-created absorption shoulder, in an attempt to clarify the roles of the confinement, contamination, and defects from an optical point of view. A comparison of the properties of these superlattice films is made with those of unlayered bulk a -SiN_x:H with different alloy composition and hydrogen-rich a -Si:H deposited at low temperatures.

II. EXPERIMENT

Superlattice samples consisting of alternating a -Si:H and a -SiN_x:H layers were prepared by the glow-discharge technique from silane and ammonia-silane mixtures (gas-phase ratio $R = [\text{NH}_3]/[\text{SiH}_4]$) at 330°C on polished Corning glass substrates in a single-chamber system.¹⁰ During preparation, the a -SiN_x:H ($R = 3.8$) layer thickness d_N was kept constant at either 17 or 30 Å, but the a -Si:H layer thickness d_S , constant for a given sample, was varied from 11 to 500 Å. The thickness of each individual sublayer was estimated from deposition rates. Unlayered a -Si:H films and a -SiN_x:H alloys were prepared under similar conditions from NH₃ and NH₃-SiH₄ mixtures but at different temperatures and gas ratios R , respectively. The composition x describes the total number of nitrogen atoms per Si atom and has been estimated as

$$x = 2R(3 + R)^{-1} \quad (1)$$

from the results of electron microprobe analysis in Ref. 23.

The experimental configuration for PDS spectroscopic investigation is shown in Fig. 1. The pump beam was a broad-band xenon arc lamp of 450 W which is dispersed by a $\frac{1}{4}$ -m grating monochromator (13 nm of resolution) and focused on the sample. The intensity of the pump beam was monitored at each wavelength and the typical chopping frequency was 20 Hz. A He-Ne laser was used as a probe beam. The samples were placed in a glass cell containing CCl₄ as a deflecting medium kept at 300 K. The probe beam deflections through the sample were measured by a position sensor (PS) detector (silicon photodiode). The lock-in amplifier, intensity monitor and monochromator were interfaced to a computer for automatic data acquisition. Deflection signal was counted for about 20 s at each pump wavelength. The interference fringes in the PDS spectra have been averaged out using conventional techniques. The photoluminescence measurements used a He-Ne (6328 Å) laser for excitation and a cooled Ge detector.

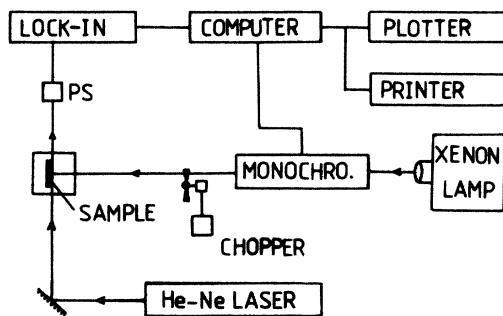


FIG. 1. Schematic diagram of the experimental setup for PDS measurements.

III. RESULTS AND DISCUSSION

Gap-state absorption spectra of the a -Si:H/ a -SiN_x:H ($x = 1.1$) superlattices are shown in Fig. 2. These samples have different a -Si:H sublayer thicknesses d_S , but each contains 40 layer pairs. The absorption coefficient $\alpha(\hbar\omega)$ of the samples was calculated using the total superlattice thickness (for each superlattice, the total a -Si:H sublayer occupies almost half of the sample volume). Spectra of the individual layers used in the fabrication of the superlattices as the quantum well and barrier layer, i.e., unlayered bulk a -Si:H and a -SiN_x:H alloy ($x = 1.1$ and the dielectric constant $\epsilon = 6.5$ as determined from transmission measurements) are also shown. The absorption in the alloy is relatively weak, so that we assume the contribution of the silicon-nitride layer to the spectra is negligible in the region of interest. Note also that, because of the saturation of the deflection signal, the high absorbance part of the PDS spectra has been completed from transmission measurements. The saturation level of the signal for the samples reported here corresponds typically to an absorption of the order of $\alpha \sim 10^4 \text{ cm}^{-1}$. The same figure also compares the spectra of the nitrogen-rich silicon-nitride alloys (dashed lines 1 and 2) with those of the superlattice samples.

Figure 2 shows that the optical absorption edges of the a -Si:H/ a -SiN_x:H superlattices are strongly blue-shifted for d_S less than 20 Å. Similar shifts have also been observed from transmission measurements.^{10,24} The optical band gap E_G from such measurements was determined using the Tauc law:

$$(\alpha\hbar\omega)^{1/2} \propto (\hbar\omega - E_G), \quad (2)$$

and E_G so obtained is plotted versus thickness in Fig. 3(a). In the calculation of $\alpha(\hbar\omega)$ for the a -Si:H layer, the effective dielectric constant of the layered structure is considered. The most striking feature of the figure is the rapid change of the band gap when the a -Si:H thickness is reduced below about 30 Å. In order to avoid possible

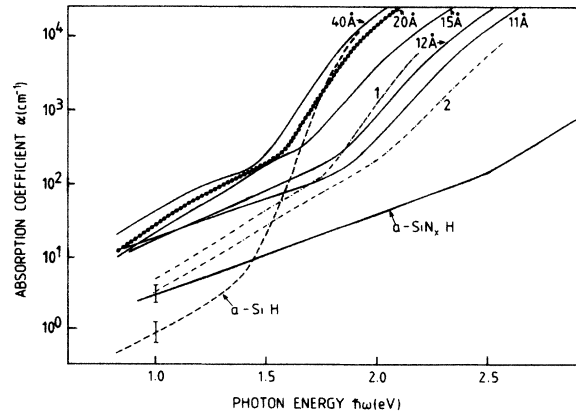


FIG. 2. Gap-state absorption of the a -Si:H/ a -SiN_x:H superlattices. Also shown are the spectra of unlayered a -Si:H and a -SiN_x:H ($x = 1.1$). In the figure, 1 and 2 indicate the spectra of a -SiN_{0.5}:H and a -SiN_{0.8}:H, respectively.

errors originating from the constant index-of-refraction Tauc formalism,²⁵ we have also plotted the E_{03} gap (energy at $\alpha=10^3 \text{ cm}^{-1}$) of the superlattices as deduced from PDS measurements. The results confirm the upward shift in the band gap. The figure indicates clearly that there is a blue-shift of the edge corresponding to an increase of the gap of at least 450 meV in the lowest-thickness superlattices. We notice also that the absorption edges and band gaps of the superlattices with larger thicknesses ($d_S > 30 \text{ \AA}$) are close to that of unlayered $a\text{-Si:H}$.

As other groups^{1,3} have observed, the main evidence for the quantum confinement effect in amorphous superlattice structures is the blue-shift of the optical band gap E_G when the confined layer thickness is decreased. The solid line in Fig. 3(a) is calculated using the Kronig-Penney model for a free electron in a one-dimensional periodic square potential well with the equation

$$\frac{\gamma^2 - \beta^2}{2\beta\gamma} \sinh(\gamma d_N) \sin(\beta d_S) + \cosh(\gamma d_N) \cos(\beta d_S) = \cos[a(d_S + d_N)], \quad (3)$$

where $\beta = (2mE)^{1/2}/\hbar$, $\gamma = [2m(V_0 - E)]^{1/2}/\hbar$; V_0 is the periodic potential field and $a = 2\pi n/d$, where n is an integer and d is the distance for one period. In the calculation, the conduction- and valence-band discontinuities, and the electron and hole effective masses are assumed to be $\Delta U_C = 1.0 \text{ eV}$, $\Delta U_V = 0.6 \text{ eV}$, $m_e^* = 0.2m_0$, and $m_h^* = 1.0m_0$, respectively, following Ref. 24. The thickness ratio of the silicon and nitride sublayers, d_S/d_N , is 0.9, and the $a\text{-Si:H}$ and $a\text{-SiN}_x\text{:H}$ band gaps are taken to be 1.7 and 3.3 eV, respectively, according to our measurements on corresponding bulk materials. We notice that the calculated optical gap is in good agreement with the experimental data. Thus the changes seen in Fig. 3(a) suggest quantization of the extended states in the $a\text{-Si:H}$ well layer as predicted by a one-dimensional quantum-well model.

The upward shift of the gap [Fig. 3(a)] is followed by a broadening of the optical absorption edge. This edge exhibits an exponential region (in the range of $200 \text{ cm}^{-1} \lesssim \alpha \lesssim 6000 \text{ cm}^{-1}$) in the characteristic Urbach form²⁶

$$\alpha(\hbar\omega) = \alpha_0 \exp[(\hbar\omega - \hbar\omega_0)/E_0], \quad (4)$$

where α_0 is the absorption at the energy $\hbar\omega_0$ and the energy E_0 is the Urbach parameter which is characteristic of the material. This exponential region extends over more than 1 order of magnitude on the absorption edge of the superlattices and increases up to 3 orders of magnitude in pure $a\text{-Si:H}$. The typical E_0 parameter of the superlattices is about 95 meV, but increases up to 130 meV in the thinnest layers [Fig. 3(b)]. Note that the change in E_0 is relatively abrupt and occurs at about the same thickness with the band gap. However, unlike the gap, the observed changes in E_0 are not readily correlated with quantum confinement effects. The increase of this parameter probably suggests an increased structural disorder in the material, as has been the case in $a\text{-Si:H}$.²⁷

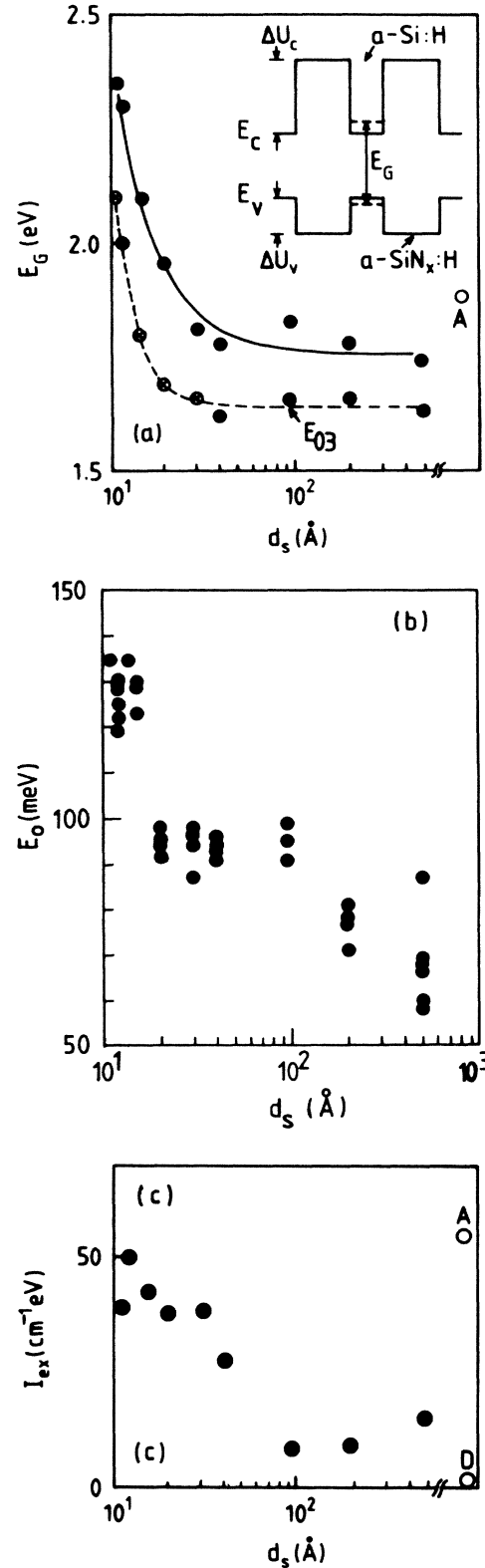


FIG. 3. (a) Thickness dependence of the optical band gap E_G (the solid line is a calculated curve based on the band diagram inserted in the same figure). Also shown is the E_{03} gap, energy at $\alpha=10^3 \text{ cm}^{-1}$, from PDS measurements, (b) the Urbach edge parameter E_0 , and (c) the integrated defect-state absorption intensity I_{ex} . Open circles (A and D) show the hydrogen rich $a\text{-Si:H}$ deposited at 40 and 300°C, respectively.

The origin of such a disorder may be the large lattice mismatch between silicon and the silicon-nitride matrix. The Raman measurements suggest an increased bond-angle distortion in the first as well as second monolayers of the well next to interfaces.²⁸ Others¹⁴ have interpreted the same effects in terms of the formation of structural defects analogous to crystalline misfit dislocations. However, the excess hydrogen and nitrogen content at interfaces or contamination of the well by these elements may also be possible sources of the Urbach edge broadening, which we will discuss later.

It has been reported that the defect-tail absorption in $a\text{-Si:H}/a\text{-SiN}_x\text{:H}$ superlattice systems increases with decreasing sublayer thickness.^{2,29} However, there is no evidence for such an increase in our spectra. The defect-tail absorption in the region below about 1.6–1.7 eV (Fig. 2) shows that the absorption coefficient $\alpha(\hbar\omega)$ at a given energy decreases slightly with thickness. The absorption in this region reveals a wider tail due to the opening of the gap. Thus the total integrated absorption I_{ex} [Fig. 3(c)] from the lowest energies to the Urbach tail increases with decreasing thickness (by a factor of 4). In the films with sublayer thicknesses $d_s < 30 \text{ \AA}$, we estimate typically $3.2 \times 10^{17} \text{ cm}^{-3}$ bulk density of states using local-field corrections made for $a\text{-Si:H}$.^{30,31} This value can be expressed as an equivalent interface state density of $8.0 \times 10^{12} \text{ cm}^{-2}$, which seems reasonable compared to ESR measurements on $a\text{-Si:H}/a\text{-SiN}_x\text{:H}$ superlattices.¹⁷ The high density of states deduced from the low-energy shoulders of the spectra suggest that these superlattices are relatively defect-rich materials.

In order to check whether the observed properties of the superlattices are due to chemical contamination of the quantum-well layer, we carried out similar optical measurements on the bulk hydrogen-rich $a\text{-Si:H}$ and nitrogen-rich $a\text{-SiN}_x\text{:H}$ grown under similar conditions.

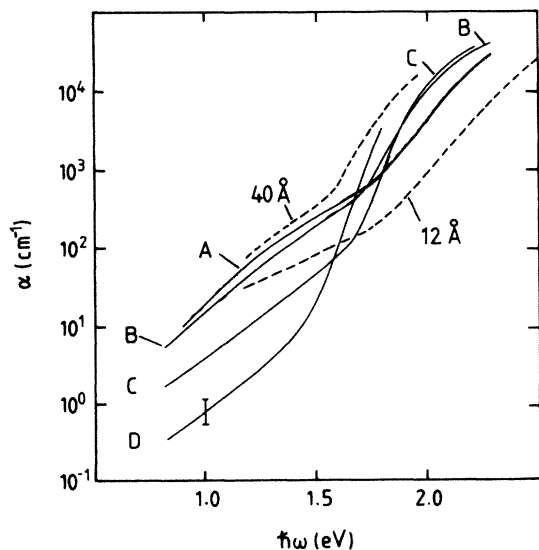


FIG. 4. Gap-state absorption of the bulk $a\text{-Si:H}$ deposited at 40 (A), 90 (B), 150 (C), and 300°C (D). Samples contain 35%, 27%, 22%, and 15% H, respectively. Also shown are the spectra of the 12- and 40-Å superlattice samples.

Figure 4 summarizes the PDS results obtained on $a\text{-Si:H}$ samples of different hydrogen quantity. Hydrogen content of the samples was estimated from the data in Ref. 32. These samples were grown at low temperature and are rich in defects and disorder like the superlattice samples. Therefore we tried to simulate the superlattices with these $a\text{-Si:H}$ samples. However, in the figure we find substantial differences between hydrogenation and size effects. Unlike the size effects (Fig. 2), the defect-state absorption at a given energy increases with hydrogenation. Moreover, the absorption edge is relatively insensitive to hydrogen content. We then conclude that, in the range of temperature explored, the superlattices cannot be simulated with these $a\text{-Si:H}$ samples. If there is any excess H content in the lowest-thickness superlattices, this may explain the relatively high density of states throughout the gap in the superlattices. But the observed changes in E_G and E_0 are probably not due to an increased hydrogen content in the quantum-well layer.

Figure 2 compares the PDS spectra of the nitrogen-rich $a\text{-SiN}_x\text{:H}$ alloys and superlattice samples. Despite the good fit at high energies between the lowest-thickness superlattices and alloys of composition range 0.5–0.8, none of the spectra fits completely those of the alloys. This clearly indicates that the lowest-thickness superlattices cannot be considered as mixed structures in the sense of forming a silicon-nitride alloy. This result is also confirmed by PL measurements. Figure 5 compares the 300-K emission spectra of the 12-Å superlattice with those of the hydrogen-rich bulk $a\text{-Si:H}$ and nitrogen-rich silicon-nitride alloy. This comparison is made because $a\text{-Si:H}$ (~35% H) and $a\text{-SiN}_x\text{:H}$ ($x=0.8$) exhibit closest optical features to the lowest-thickness superlattices. The figure shows that, unlike $a\text{-Si:H}$ and the silicon-nitride alloy, the emission spectrum of the superlattice sample consists of the two bands situated at 1.3 and 1.46 eV. The band at lower energy is the typical emission band of the bulk $a\text{-Si:H}$, which occurs from the radiative recombina-

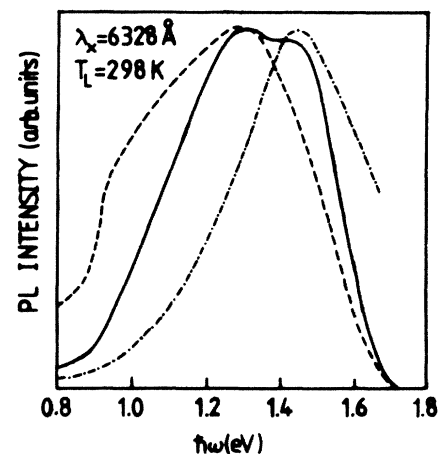


FIG. 5. Normalized PL spectra of 12-Å superlattice (—), hydrogen-rich $a\text{-Si:H}$ (35% H) (---) and $a\text{-SiN}_{0.8}\text{:H}$ alloy (-.-.-).

tion of the electrons and holes in the band-tail states. Also, by analogy with the nitrogen-rich silicon-nitride alloys, we ascribe the emission band at 1.46 eV to the nitrogen-rich regions of the superlattice. These regions are probably formed at interfaces during the growth of the $a\text{-SiN}_x\text{:H}$ layer on $a\text{-Si:H}$. Because of the reactive nature of the plasma, we suppose that the weak Si—H bonds (71.5 kcal/mol) of the $a\text{-Si:H}$ surface are replaced by the strong Si—N bonds (105 kcal/mol) (Ref. 33) resulting in the nitrogen-rich regions. The 1.3-eV emission band can also be explained by the existence of the hydrogen-rich interfaces ($a\text{-Si:H}$ on $a\text{-SiN}_x\text{:H}$). The photoluminescence spectra then arise probably from the tunneling of the electrons and holes to these asymmetric interface states. The hydrogen- and nitrogen-rich interfaces have also been suggested by other groups.^{13,34,35}

In summary, we have investigated the optical properties of the $a\text{-Si:H}/a\text{-SiN}_x\text{:H}$ ($x = 1.1$) superlattices as a function of the $a\text{-Si:H}$ sublayer thickness using photo-thermal deflection and photoluminescence spectroscopies. We have demonstrated the quantum size effects

from the blue-shift of the fundamental absorption edge when the sublayer thickness is reduced below about 30 Å. It is shown that, although there are close features in the optical properties of the superlattice samples and $a\text{-SiN}_x\text{:H}$ alloys, even the smallest-thickness superlattices cannot be considered as a silicon-nitride alloy. We have shown that the 300-K emission of the lowest-thickness superlattice samples consist of the two bands, which we attributed to the presence of the hydrogen- and nitrogen-rich interfaces. The exclusion of the nitrogen and hydrogen effects should clearly demonstrate the existence of the quantum size effects in these amorphous superlattice structures.

ACKNOWLEDGMENTS

I wish to thank the late Professor I. G. Austin and the University of Sheffield for provision of research facilities, and Professor W. E. Spear, and co-workers at the University of Dundee, for providing samples. I am also indebted to the Science and Engineering Research Council (SERC) of the United Kingdom for its financial support.

*Present address: Coordinated Science Laboratory, University of Illinois at Urbana-Champaign, 1101 West Springfield Avenue, Urbana, Illinois 61801-3082.

¹B. Abeles and T. Tiedje, *Phys. Rev. Lett.* **51**, 2003 (1983).

²N. Ibaraki and H. Fritzsche, *Phys. Rev. B* **30**, 5791 (1984).

³M. Hirose and S. Miyazaki, *J. Non-Cryst. Solids* **66**, 327 (1984).

⁴P. V. Santos, L. Ley, J. Mebert, and O. Koblinger, *Phys. Rev. B* **36**, 4858 (1987).

⁵A. T. Snell, K. D. Mackenzie, W. E. Spear, P. G. LeComber, and A. J. Hughes, *Appl. Phys. A* **24**, 357 (1981).

⁶N. B. Goodman and H. Fritzsche, *Philos. Mag. B* **42**, 149 (1980).

⁷C. Ogihara, H. Takenaka, K. Morgaki, S. Nitta, S. Miyazaki, and M. Hirose, *Solid State Commun.* **61**, 431 (1987).

⁸R. Dingle, W. Wiegmann, and C. H. Henry, *Phys. Rev. Lett.* **33**, 827 (1974).

⁹S. Kalem, M. Hopkinson, T. M. Searle, I. G. Austin, W. E. Spear, and P. G. LeComber, in *Proceedings of the 18th International Conference on the Physics of Semiconductors, Stockholm, 1986*, edited by O. Engstrom (World-Scientific, Singapore, 1987), Vol. 1, p. 747.

¹⁰P. G. LeComber, W. E. Spear, R. A. Gibson, M. Hopkinson, P. K. Bhat, T. M. Searle, and I. G. Austin, *J. Non-Cryst. Solids* **77&78**, 1081 (1985).

¹¹P. Santos, M. Hundhausen, and L. Ley, *J. Non-Cryst. Solids* **77&78**, 1069 (1985).

¹²H. T. Grahn, H. A. Stoddart, T. Zhou, Z. Vardeny, J. Tauc, and B. Abeles, in *Proceedings of the 18th International Conference on the Physics of Semiconductors*, Ref. 9, Vol. 2, p. 1037.

¹³B. Abeles, P. D. Persans, H. S. Stasiewski, L. Yang, and W. Lanford, *J. Non-Cryst. Solids*, **77&78**, 1065 (1985).

¹⁴C. B. Roxlo, B. Abeles, and T. Tiedje, *Phys. Rev. Lett.* **52**, 1994 (1984).

¹⁵R. Cheng, S. Wen, J. Feng, and H. Fritzsche, *J. Non-Cryst. Solids* **77&78**, 1061 (1985).

¹⁶L. Yang, B. Abeles, and P. D. Persans, *Appl. Phys. Lett.* **49**, 631 (1986).

¹⁷C. C. Tsai, M. J. Thompson, R. A. Street, M. Stutzmann, and F. Ponce, *J. Non-Cryst. Solids* **77&78**, 995 (1985).

¹⁸C. B. Roxlo and B. Abeles, *Phys. Rev. B* **34**, 2522 (1986).

¹⁹J. R. Abelson, C. C. Tsai, and T. W. Sigmon, *Appl. Phys. Lett.* **49**, 850 (1986).

²⁰I. G. Austin, W. A. Jackson, T. M. Searle, P. K. Bhat, and R. A. Gibson, *Philos. Mag. B* **52**, 271 (1985).

²¹B. A. Wilson, C. M. Taylor, and J. P. Harbison, *Phys. Rev. B* **34**, 8733 (1986).

²²W. B. Jackson, N. M. Amer, A. C. Boccara, and D. Fournier, *Appl. Opt.* **20**, 1333 (1981).

²³B. Dunnett, P. G. LeComber, and W. E. Spear, *Philos. Mag. A* (to be published).

²⁴B. Abeles and T. Tiedje, in *Semiconductors and Semimetals*, edited by J. I. Pankove (Academic, New York, 1984), Vol. 21, Pt. C, p. 407.

²⁵R. W. Collins and C.-Y. Huang, *Phys. Rev. B* **34**, 2910 (1986).

²⁶F. Urbach, *Phys. Rev.* **92**, 1324 (1953).

²⁷G. D. Cody, in *Semiconductors and Semimetals*, Ref. 24, Vol. 21, Pt. B.

²⁸N. Maley and J. S. Lannin, *Phys. Rev. B* **31**, 5577 (1985).

²⁹T. Tiedje and B. Abeles, *Appl. Phys. Lett.* **45**, 179 (1984).

³⁰M. H. Brodsky, M. Cardona, and J. J. Cuomo, *Phys. Rev. B* **16**, 3556 (1977).

³¹W. B. Jackson and N. M. Amer, *Phys. Rev. B* **25**, 5559 (1982).

³²W. Beyer, in *Tetrahedrally-Bonded Amorphous Semiconductors*, edited by D. Adler and H. Fritzsche (Plenum, New York, 1985), p. 129.

³³*Handbook of Chemistry and Physics*, 65th ed., edited by Robert C. Weast *et al.* (CRC, Florida, 1987), pp. F169–172.

³⁴R. W. Collins, *J. Appl. Phys.* **60**, 1377 (1986).

³⁵M. Hundhausen, P. Santos, L. Ley, F. Habraken, W. Beyer, R. Primig, and G. Gorges, *J. Appl. Phys.* **61**, 556 (1987).